Progress In Electromagnetics Research C, Vol. 54, 103–116, 2014

Design of CPW-Fed Dual-Band Printed Monopole Antennas for LTE/WiMAX/WLAN and UWB Applications

Praveen V. Naidu[1] and Raj Kumar[2, *]

Abstract—In this paper, two miniaturized ($20 \times 20\,\text{mm}^2$) coplanar waveguide fed slot antennas are proposed. Both the antennas are characterized by ultra wide impedance bandwidth while one of them has an additional narrow band near 2.5 GHz. The radiating element of the proposed antennas is a modified rectangular geometry which is excited by a 50 ohm line. The slot in the ground plane is stair case shape for UWB antenna and octagonal shape for the dual-band antenna. By modifying the slot and adding a $\lambda/4$ length metallic stub, an extra resonance is created for the dual-band antenna. The measured impedance bandwidth of the UWB antenna is 7.8 GHz (3.4–11.2 GHz). The impedance bandwidths of the dual-band antenna are 150 MHz (2.45–2.6 GHz) and 8.4 GHz (3.2–11.6 GHz). The radiation patterns of the proposed antenna are found to be bi-directional in E-plane and omni-directional in H-plane. All the measured and simulated results are in good agreement.

1. INTRODUCTION

The rapid progress in the development of short range, ultra-fast wireless communication systems started only after the allocation of an unlicensed frequency band from 3.1 to 10.6 GHz by the Federal Communication Commission [1] in 2002. Design of compact multi-band antennas for portable wireless communication systems is quite a challenging task because it has to satisfy requirements such as wider impedance bandwidth, omnidirectional radiation pattern, constant gain, high radiation efficiency, compact size, less weight and ease of fabrication. The aforementioned characteristics can be achieved by CPW-fed antennas. Coplanar waveguide (CPW) feed besides giving a larger bandwidth allows for less dispersion, low radiation loss and good omnidirectional radiation patterns with moderate gains. In addition, the absence of via-hole connections and small ground plane requirements ensure reduced cost and system complexity and facilitate easy integration with the adjacent radio frequency (RF) circuitry.

Various CPW-fed dual-band and UWB monopole antennas [2–32] with different configurations for size reduction, bandwidth enhancement and resonance mode realization have been reported in the literature. A $30 \times 30\,\text{mm}^2$ antenna was proposed in [2] for an impedance bandwidth of 3.1–8.3 GHz. The radiating element was a trapezoid-shaped patch excited using a CPW feed. In [3], a $30 \times 20\,\text{mm}^2$ printed CPW-fed meandered patch antenna for dual-band operation was proposed. A compact $20 \times 15.5\,\text{mm}^2$ CPW-fed monopole antenna using two strips for dual-band wireless local area network (WLAN) operations was proposed in [4] giving bandwidth from 2.4 to 2.484 GHz and 5.15 to 5.825 GHz. A $30 \times 30\,\text{mm}^2$ antenna was proposed in [5] for an impedance bandwidth of 3.1–8.3 GHz. The radiating element was a trapezoidal shaped patch excited using a CPW feed. In [6], a $30 \times 25\,\text{mm}^2$ printed rectangular shaped patch with two types of shaped slots and excited by a CPW-feed line was proposed for dual-band operation from 2.34 to 2.55 GHz and from 4.8 to 9.85 GHz. In [7], A $41.6 \times 28.38\,\text{mm}^2$ CPW- fed planar monopole antenna composed of a circular radiating patch with a smiling slot for dual-band operation was presented. The antenna achieved dual impedance bandwidths from 2.3 to 3.0 GHz

Received 10 July 2014, Accepted 16 October 2014, Scheduled 23 October 2014

* Corresponding author: Raj Kumar (dr.rajkumarkumar@yahoo.com).

[1] Centre for Radio Science Studies, Department of E&TC, Symbiosis International University, Lavale, Pune 411042, India.

[2] Department of AE, ARDE, Pashan, Pune 411021, India.

and 4.7 to 5.9 GHz. A rectangular notch cut on a rectangular shaped patch CPW-feed antenna operating at 2.4 GHz and 5.2/5.8 GHz was proposed in [8]. In [9], a $21 \times 28\,\text{mm}^2$ coplanar-waveguide (CPW)-fed ultra-wideband antenna with dual band-notch characteristic was presented. The proposed antenna has two notches between 5 to 6 GHz and 7.7–8.5 GHz in the impedance bandwidth from 3.1–10.6-GHz. A $26 \times 30\,\text{mm}^2$ printed CPW-fed ultra wideband antenna with C-shaped slots on the rectangle radiator for dual-band notch characteristics was presented in [10]. A $25 \times 25\,\text{mm}^2$ CPW fed slot antenna was designed for UWB applications with band notch in the WLAN band of 5.04–6.08 GHz [11]. To achieve the band-notch characteristics, a M-shape slot was cut in the semi-circular radiating patch. In [12], a $30 \times 30\,\text{mm}^2$ ultra wideband antenna with dual notch characteristics was proposed. Two symmetrical slots are etched from the ground plane to achieve the notched band at 5.5 GHz and the other notched band at 3.5 GHz is obtained by etching a split ring slot in the radiator. In [13], a $28.5 \times 33.5\,\text{mm}^2$ CPW-fed fractal slot antenna for WLAN/WiMAX applications was discussed. It was shown to achieve an impedance bandwidth from 2.38 to 3.95 GHz and 4.95 to 6.05 GHz. A $32 \times 16\,\text{mm}^2$ ring monopole antenna with double meander lines for dual-band operation was presented in [14]. An asymmetric slot antenna with meandered slit is proposed in [15] for dual-frequency operation. In [16], an UWB antenna is designed by using the fractal concept. Again, the reported antenna is having the drawback of larger size ($77 \times 55\,\text{mm}^2$). In Table 1, a comparison of various other single and dual-band antennas [17–32] is made in terms of the antenna size, antenna purpose, bandwidth and average peak gain. From the table, it is seen that the proposed antenna is more compact ($20 \times 20\,\text{mm}^2$), has a wider impedance bandwidth and an acceptable peak gain for UWB applications. Also, the CPW feeding makes the structure uniplanar, simple to design and have less cost of fabrication (one side printing).

The dual-band and UWB monopole antennas proposed in this article are for LTE/WiMAX/WLAN and UWB applications. The proposed UWB antenna provides an impedance bandwidth of 7.8 GHz, and the proposed dual-band antenna provides impedance bandwidths of 150 MHz and 8.3 GHz. The antenna's performance was simulated using CST Microwave Studio. The effect of antenna's key structural parameters on its performance was also analyzed.

Table 1. Comparison of reference antennas in terms of size, bandwidth and peak gain.

Published literature	Antenna Purpose	Antenna Size	Bandwidth	Average peak gain
Ref. [17]	Single-band	$100 \times 100\,\text{mm}^2$	3.1–10.6 GHz	∼3 dBi
Ref. [18]	Single-band	$120 \times 100\,\text{mm}^2$	3.1–10.6 GHz	∼3.5 dBi
Ref. [19]	Single-band	$45 \times 21.5\,\text{mm}^2$	3.0–10 GHz	∼4 dBi
Ref. [20]	Single-band	$40 \times 100\,\text{mm}^2$	3.1–5.15 GHz	∼3 dBi
Ref. [21]	Single-band	$66.1 \times 44\,\text{mm}^2$	3.1–12 GHz	∼3 dBi
Ref. [22]	Single-band	$85 \times 85\,\text{mm}^2$	2.8–14 GHz	∼6 dBi
Ref. [23]	Single-band	$90 \times 90\,\text{mm}^2$	4.71–6.14 GHz	∼3.3 dBi
Ref. [24]	Single-band	$85 \times 85\,\text{mm}^2$	2.85–15.12 GHz	∼6 dBi
Ref. [25]	Single-band	$100 \times 100\,\text{mm}^2$	2.79–9.48 GHz	∼2.5 dBi
Ref. [26]	Single-band	$50 \times 42\,\text{mm}^2$	2.78–9.78 GHz	∼1.5 dBi
Ref. [27]	Dual-band	$45 \times 32\,\text{mm}^2$	2.4–2.5 GHz and 3.1–10.6 GHz	-
Ref. [28]	Dual-band	$42 \times 46\,\text{mm}^2$	2.4–2.484 GHz and 3.1–10.6 GHz	∼4 dBi
Ref. [29]	Dual-band	$60 \times 60\,\text{mm}^2$	2.25–2.53 GHz and 5.13–5.99 GHz	∼4.8 dBi
Ref. [30]	Dual-band	$75 \times 75\,\text{mm}^2$	2.4–2.484 GHz and 5.150–5.950 GHz	∼4 dBi
Ref. [31]	Dual-band	$50 \times 24\,\text{mm}^2$	2.4–2.484 GHz, 3.1–5.15 GHz and 5.825–10.6 GHz	1–4 dBi
Ref. [32]	Dual-band	$60 \times 45\,\text{mm}^2$	2.26–2.57 GHz and 4.81–6.56 GHz	2.5–3.6 dBi
Proposed work	Dual-band and Single-band	$20 \times 20\,\text{mm}^2$	2.45–2.6 GHz and 3.18–11.6 GHz	∼4 dBi

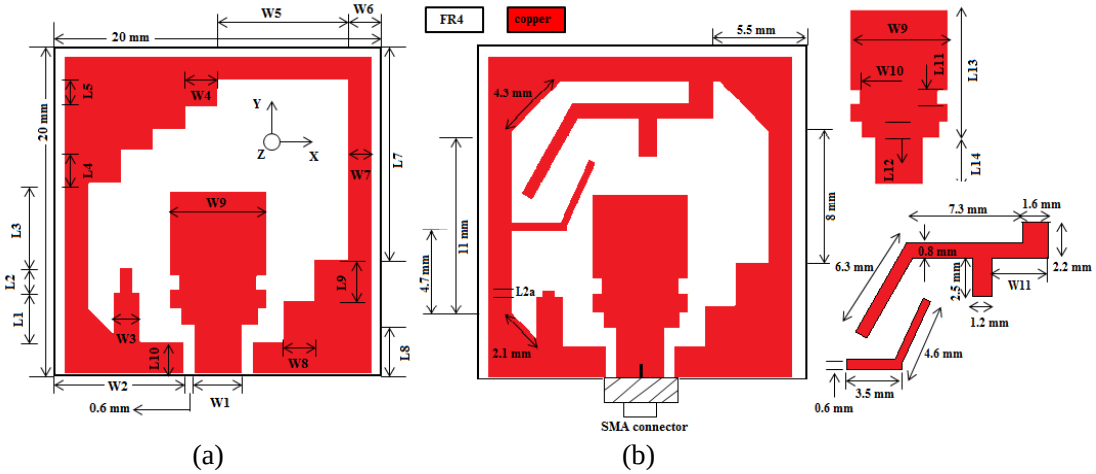

Figure 1. Structure of the proposed (a) UWB antenna (b) dual-band antenna.

Table 2. Final parameter values of the proposed antenna.

Parameter	L_1	L_2	L_3	L_4	L_5	L_{12}	L_{2a}
Value (mm)	3	1.5	5.2	2	1.6	1	0.4
Parameter	L_7	L_8	L_9	L_{10}	L_{11}	L_{13}	L_{14}
Value (mm)	13	3	2.5	2	0.6	8.2	3
Parameter	W_1	W_2	W_3	W_4	W_5	W_6	W_7
Value (mm)	3	7.4	1.7	2	8	2	1.5
Parameter	W_8	W_9	W_{10}	W_{11}			
Value (mm)	2	6	0.6	3.5			

2. ANTENNA DESIGN

The structures of the proposed CPW-fed antennas are shown in Figure 1. The antenna is printed on one side of a low-cost dielectric substrate (FR4) with thickness of 1.6 mm, relative permittivity of 4.4 and loss tangent of 0.018. Initially, an octagonal slot is etched in the ground plane. The slot is excited by a 50 ohms line terminated on a modified rectangular patch. The impedance bandwidth obtained with this configuration is large. To further increase the impedance bandwidth, the shape of the slot in the ground plane is changed step by step by observing the reflection coefficient characteristics. Finally with staircase slot, the UWB performance is obtained. The extra stub in the ground plane is added to increase the coupling between the slot and the radiating patch, and results into better impedance matching. Next, to introduce an extra resonance at 2.5 GHz, a $\lambda/4$ strip is added to the ground plane. But adding the strip affects the coupling between the ground plane and the radiating patch. To enhance the coupling, the shape of the slot is further changed and made octagonal again. Finally, the antenna configuration is optimized. The optimized dimensions of both the antennas are given in Table 2.

3. EVOLUTION STEPS OF ANTENNA

3.1. Single-band Antenna

Figure 2(a) shows the return loss characteristics for the evolutionary stages of the ultra wideband antenna. As described in the antenna geometry, the initial design is an octagonal slot containing a modified rectangular patch. The bandwidth achieved with this design is from 3 GHz to 5.2 GHz. By assigning a staircase profile to one of the corners of the slot, the bandwidth is extended to 6.8 GHz. In

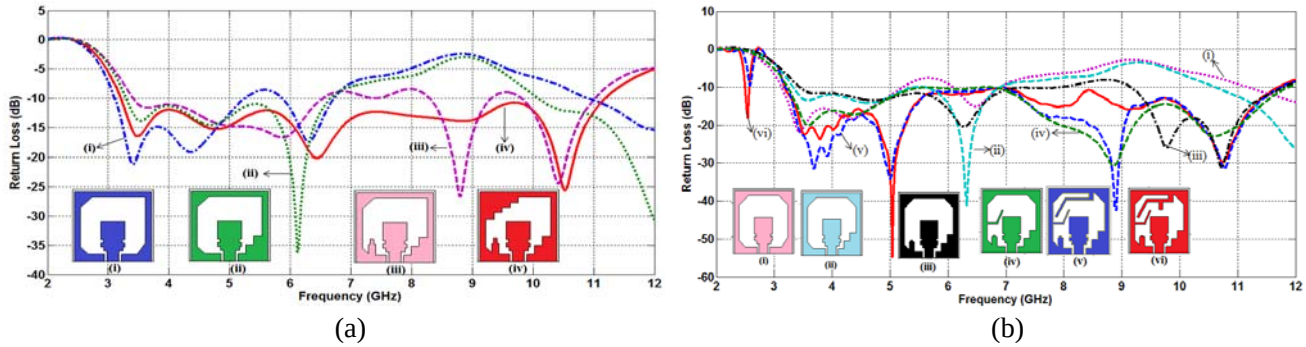

Figure 2. (a) Simulated return loss against frequency for different stages of the UWB antenna. (b) Simulated return loss against frequency for different stages of the dual-band antenna.

the third step, a small vertical stub is attached on the left side of the lower ground plane. This creates a resonance near 8.5 GHz and the bandwidth nearly covers the entire FCC UWB. Finally, the impedance matching over the entire UWB is improved by staircase profiling the upper left corner of the slot. The staircase profiling accumulates currents at its corners which creates an inductive reactance. This inductive reactance neutralizes to some extent the capacitive reactance of the slot over some frequencies and hence reduces the imaginary part of the antenna impedance. Thus, the impedance matching is improved.

3.2. Dual-band Antenna

The evolution of the dual-band antenna is shown in Figure 2(b). As for the ultra wideband antenna, progressive improvement in the impedance bandwidth can be noted with each modification. In order to keep the reflection coefficient below −10 dB for the entire ultra wide-band range a stub has been added to the ground plane nearer to the radiating patch (black color (iii)), this leads to a wider bandwidth from 3.2–11.6 GHz. Next, in order to generate a new resonant frequency near 2.5 GHz without disturbing UWB performance, narrow rectangular stub has been attached to the upper ground plane (blue color (v)). This results in a dual-frequency operation from 2.45–2.6 GHz and 3.18–11.6 GHz. It is further seen from the figure that in the final stage, to the horizontal strip attached to the ground plane at the top of the slot, a small vertical stub is attached. This makes the horizontal strip draw a larger current from the ground plane and increases the depth of the resonance at 2.5 GHz.

4. RESULTS AND DISCUSSION

The proposed antenna is designed using the commercial electromagnetic software CST Microwave Studio and fabricated with optimized dimensions. Figures 3 and 4 show the fabricated prototype along with the measured and simulated reflection coefficients for UWB antenna and dual-band antenna, respectively. The measurements have been performed using Rohde & Schwarz Vector Network Analyzer (R&S ZVA-40). As seen from Figures 3 and 4, a good agreement between the simulated and the measured results is observed. The small difference between the measured and simulated results is due to the effect of uncertainty in substrate dielectric constant, SMA connector quality and fabrication tolerance. The measured impedance bandwidth of UWB antenna is 7.8 GHz from 3.4 to 11.2 GHz and the measured impedance bandwidths of the dual-band antenna are 150 MHz from 2.45 to 2.6 GHz and 8.3 GHz from 3.2 to 11.5 GHz.

The resonance behavior of the antennas can be better understood by considering the current distribution. Figure 5 shows the surface current distribution of the UWB antenna at different frequencies. From the figure it can be concluded that the resonance at 3.5 GHz is due to the slot in the ground plane as it shows two maxima along the slot length. The resonance at 4.5 GHz is due to the modified rectangular patch as it shows maximum current on the patch. The resonance at 6.5 GHz is the second resonance of 3.5 GHz as it shows four current maxima around the slot.

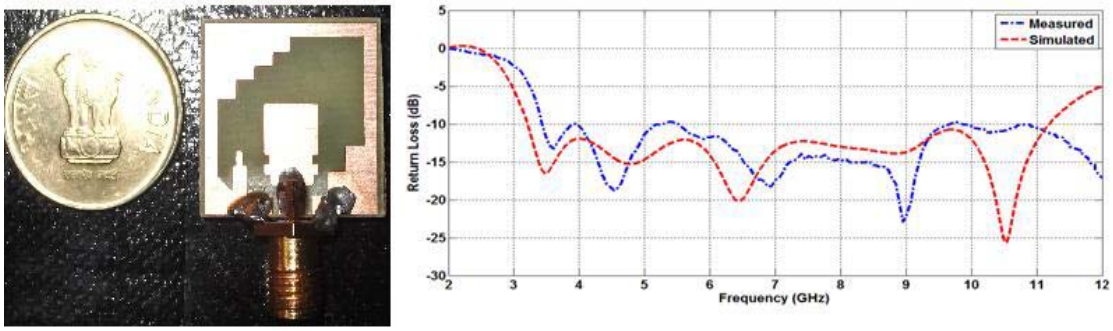

Figure 3. Fabricated component photograph along with simulated and measured return loss of the proposed UWB antenna.

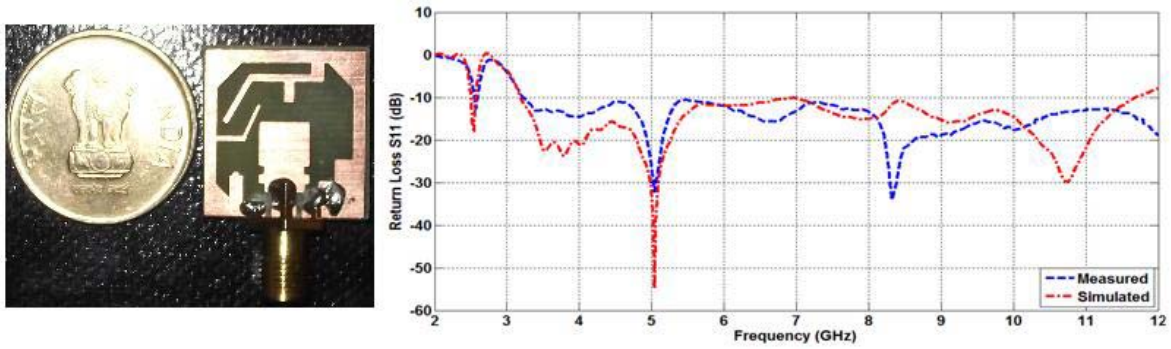

Figure 4. Fabricated component photograph along with simulated and measured return loss of the proposed dual-band antenna.

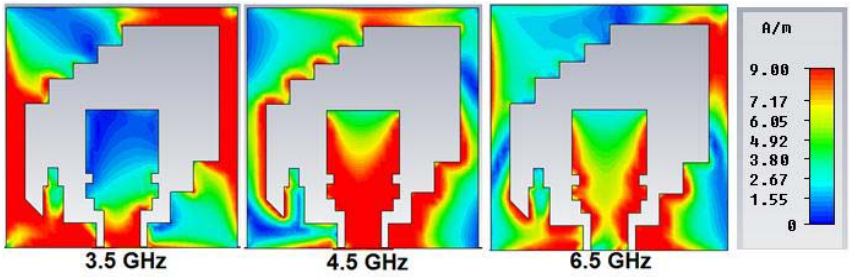

Figure 5. Current distribution at different resonance frequencies of UWB antenna.

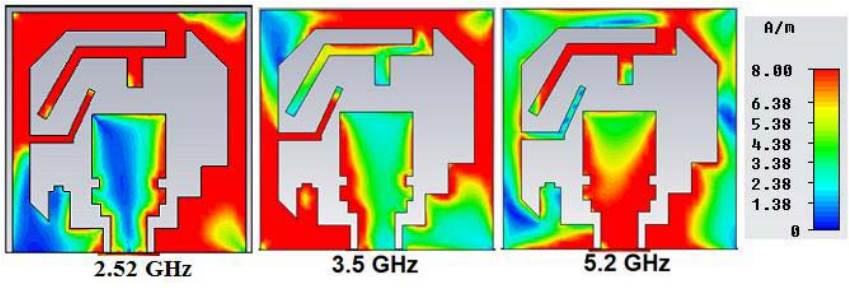

Figure 6. Current distribution at different resonance frequencies of dual-band antenna.

Figure 6 shows the current distribution of the dual-band antenna. From the figure, it can be said that the resonance at 2.52 GHz is due to the additional strip added in the ground plane. The surface current distribution shows two maxima along the slot length at 3.5 GHz and therefore the resonance at 3.5 GHz is due to the slot in the ground plane. The lower cut-off frequency of the UWB depends on the slot periphery. There is maximum current in the rectangular patch at 5.2 GHz; therefore the resonance at 5.2 GHz is due to the rectangular radiating patch. Thus, the third resonance f_3 is due to the monopole like behavior of the hexagonal patch.

5. PARAMETRIC STUDY

As discussed earlier, the first resonance in case of the dual band antenna at 2.52 GHz is due to the additional strip added to the ground plane. The resonance frequency is decided by the length X of the additional strip. The effect of this length X on the return loss of the dualband antenna is shown in Figure 7. From the figure, it can be seen that as the length X increases the first resonance shifts towards the lower frequency side. As an open ended strip line works like a $\lambda/4$ resonator, by equating the length X to $\lambda/4$, the resonance frequency can be calculated.

The importance of vertical stub on the left side of the lower ground plane in the case of proposed UWB antenna is shown in Figure 8(a). It is seen that when the vertical stub is not attached (blue color dashed-line) to the ground plane, the impedance bandwidth is only limited to 4 GHz (3.2–7.2 GHz). In order to extend and achieve full UWB, a vertical stub is attached (red color solid-line) to the ground plane so that an extra resonance can be generated at higher frequency (around 8.5 GHz). The simulated current distribution at 8.5 GHz shown as an inset in Figure 8(a) confirms this resonance. Further, this stub increases the coupling between the patch and the ground plane and a wider bandwidth is achieved from 3.2–11.2 GHz.

Figure 8(b) shows the effect of variation of L_{2a} on the return loss of the dual-band antenna. It can be seen from the figure that length L_{2a} has a significant effect on the return loss. As the value of L_{2a} increases or decreases from a particular value, the return loss starts deteriorating. Therefore, there is a need of optimization of the value of L_{2a}, which is optimized and found to be 0.4 mm.

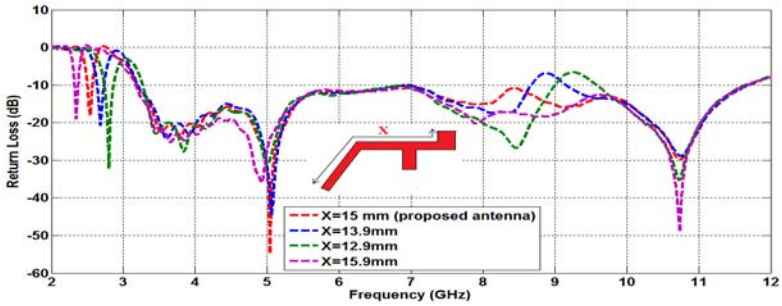

Figure 7. Effect of parameter length X on the return loss of the proposed dual-band antenna.

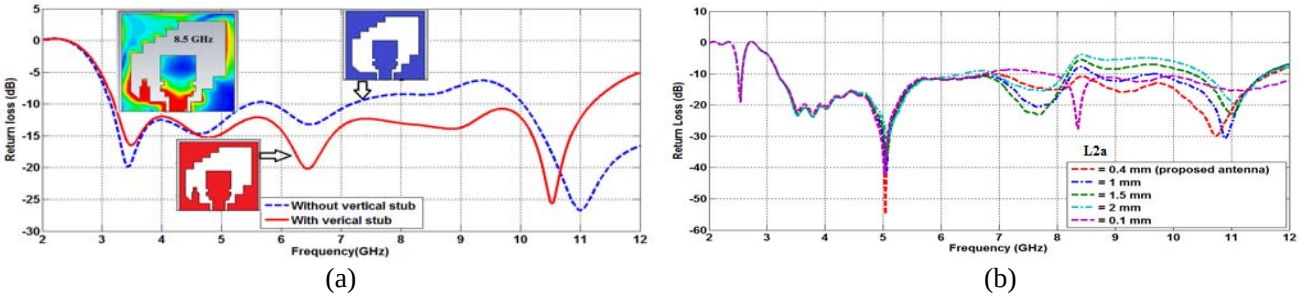

Figure 8. (a) Simulated S_{11} for antenna with and without vertical stub. (b) Effect of parameter length L_{2a} on the return loss of the proposed dual-band antenna.

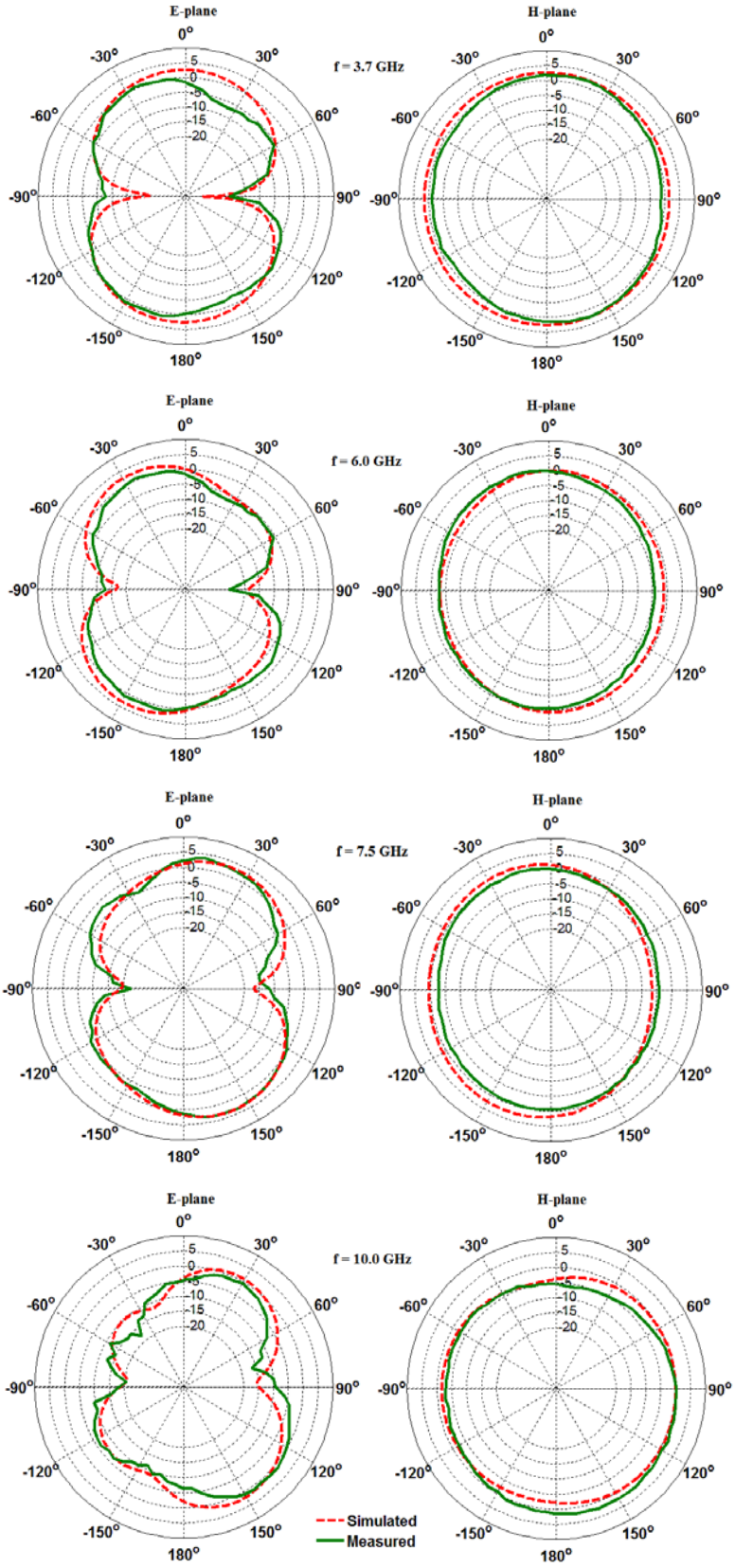

Figure 9. Radiation patterns of UWB antenna at 3.7 GHz, 6.0 GHz, 7.5 GHz and 10 GHz.

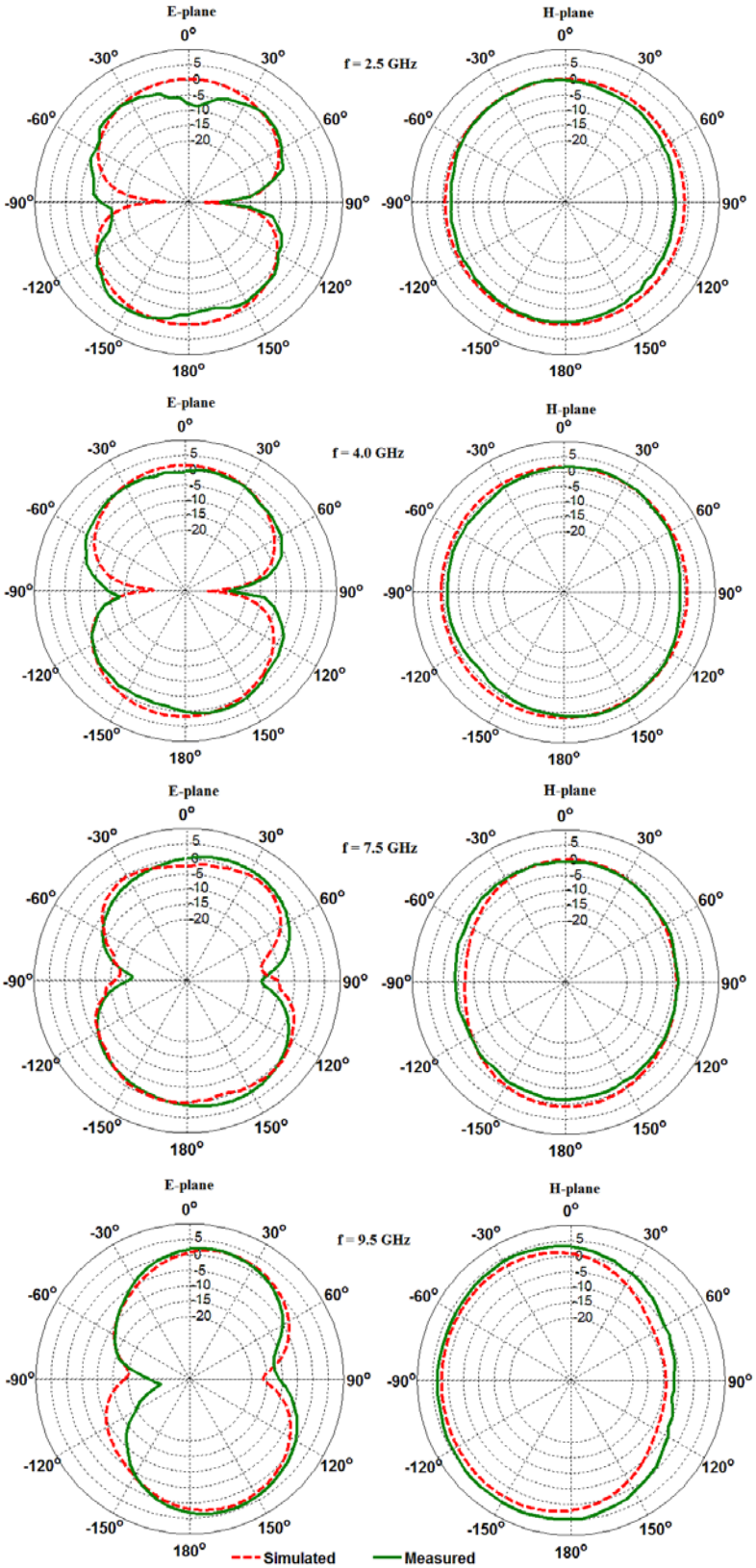

Figure 10. Simulated and measured radiation patterns at 2.5 GHz, 4.0 GHz, 6.0 GHz, 7.5 GHz and 9.5 GHz of the dual-band antenna in the E-plane and H-plane.

6. RADIATION PATTERNS AND PEAK GAIN

The radiation patterns of the proposed two antennas are simulated in E-plane and H-plane using CST Microwave Studio and measured in an anechoic chamber using antenna measurement system. A standard double-ridged horn is used as a reference antenna. The simulated and measured radiation patterns of the proposed antenna at different frequencies are shown in Figures 9 and 10. The H-plane radiation pattern has omni-directional shape while the E-plane radiation pattern has bidirectional or dumb bell shape. For both the cases, the simulated and measured results are found to be in close agreement with a little difference due to measurement and alignment errors. At higher frequencies, the radiation pattern deteriorates because the equivalent radiating area changes with frequency over UWB. Unequal phase distribution and significant magnitude of higher order modes at higher frequencies also play a part in the deterioration of radiation pattern at higher frequencies.

In Figure 11, the simulated radiation patterns for the antenna without the staircase profile and the proposed antenna (antenna with the staircase profile) are compared. It is noted from the figure that by introducing the staircase profile, a slight asymmetry is introduced in the radiation patterns.

The measured peak gains of the proposed antennas as functions of frequency in the operating band are plotted in Figure 12. As can be seen, stable gains across the desired bands have been achieved. The peak gain remains between 1 and 8 dBi in the useful band and increases with frequency due to the increased effective area of the antenna at shorter wavelengths. The stable radiation patterns with a reasonable peak gain make the proposed antenna suitable for being used in LTE/WiMAX/WLAN and UWB communication applications.

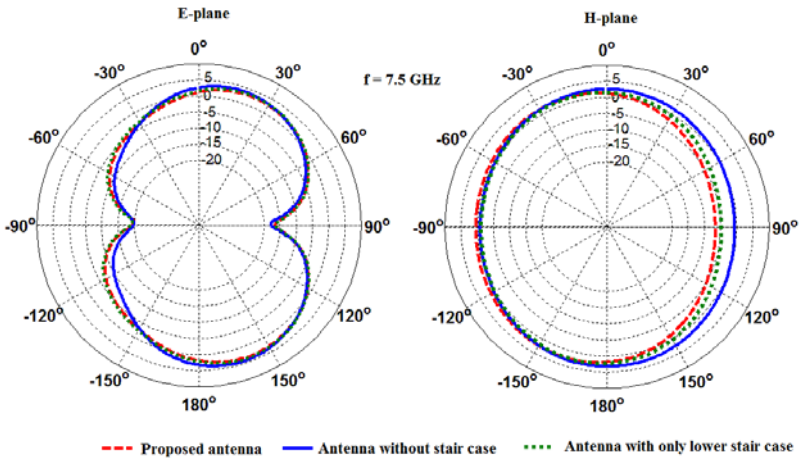

Figure 11. Simulated radiation patterns at 7.5 GHz for the UWB antenna with and without staircase profiling.

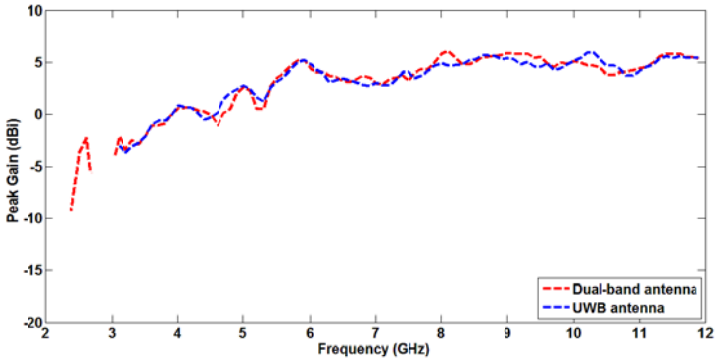

Figure 12. Measured peak gain of the proposed antennas.

7. ANTENNA DESIGN WITH BAND-NOTCH CHARACTERISTICS

To minimize the interference of the antenna with existing 5.1–5.85 GHz WLAN band, the antenna design is slightly modified to generate an impedance notch near 5.5 GHz. The modified design is shown in Figure 13. As seen in the figure, an open ring slot is etched on the radiating patch to create the desired characteristics. The width of the slot is 0.3 mm while the mean length of the slot is made equal to 17 mm. The slot resonates at the frequency where its length becomes equal to half of the wavelength. Hence for a length of 17 mm, the resonance frequency using Equation (1) comes out to be 5.4 GHz.

$$f \text{ (in GHz)} = \frac{C}{2(\text{ring slot length})\sqrt{\varepsilon_{r,eff}}} \tag{1}$$

$$\varepsilon_{r,eff} = \frac{\varepsilon_r + 1}{2} \tag{2}$$

In Figure 14, the simulated reflection coefficients for the antenna with and without band notch characteristics are shown. Comparison is made for both the cases, the ultra wideband antenna and the dual-band antenna. It is seen that with the introduction of the slot on the patch, a notched band is realized in 5–6 GHz band. From the simulated VSWR plot (Figure 15), it can be seen that the VSWR in the notched band reaches up to 8 for the UWB design while for the dual-band design, it crosses the value of 12. To see how the location of the notch varies with the length of the ring slot on the patch, a small parametric study is performed for the UWB antenna, and the dual-band antenna and the results

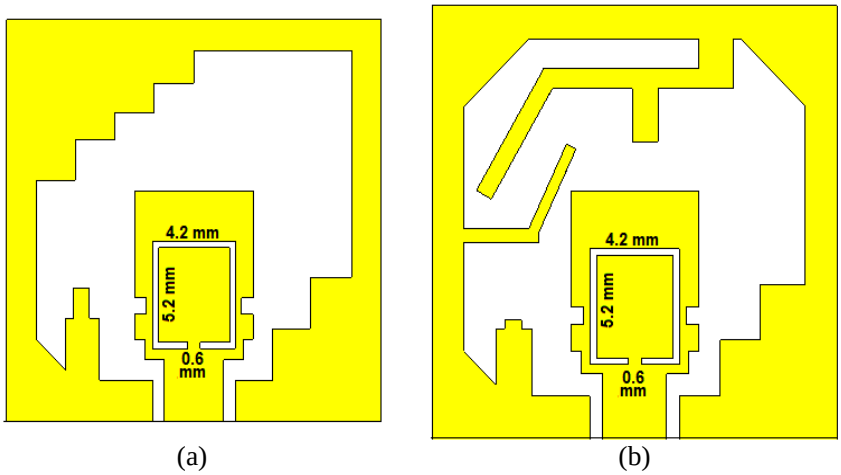

Figure 13. Geometry of the antennas for the band-notch characteristics. (a) UWB antenna. (b) Dual-band antenna.

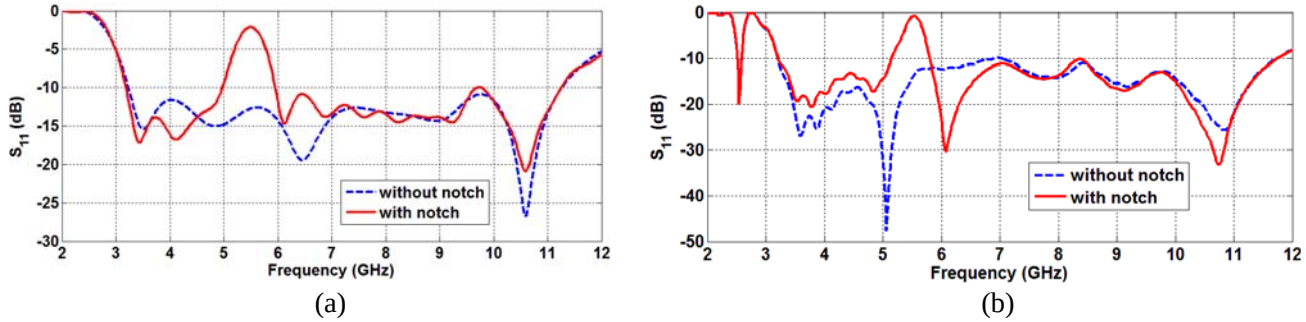

Figure 14. (a) Simulated S_{11} with and without band notch characteristics for (a) UWB design and (b) dual-band design.

are shown in Figure 16. It can be noted as expected that as the length of the slot is increased, the notch frequency decreases.

The simulated surface current distribution for the two antenna designs with notched characteristics (UWB and dual band) is shown in Figure 17 and Figure 18 respectively. The current distribution is shown at two frequencies; one within the notched band (5.5 GHz) and one outside of the notched band (7.0 GHz). It can be seen from the figure that for both the antennas, there is a significantly higher current distribution around the open ring slot at the in-band frequency (5.5 GHz) when compared to the current distribution at 7.0 GHz. When the slot resonates, it acts as a short circuit to the feed line absorbing most of the current, dissipating it in the form of conductor loss and leaving little power for radiation.

The peak gains of the proposed UWB and dual-band antenna with notch characteristics as obtained from CST Microwave Studio simulations are given in Figure 19. It can be observed from Figure 19(a)

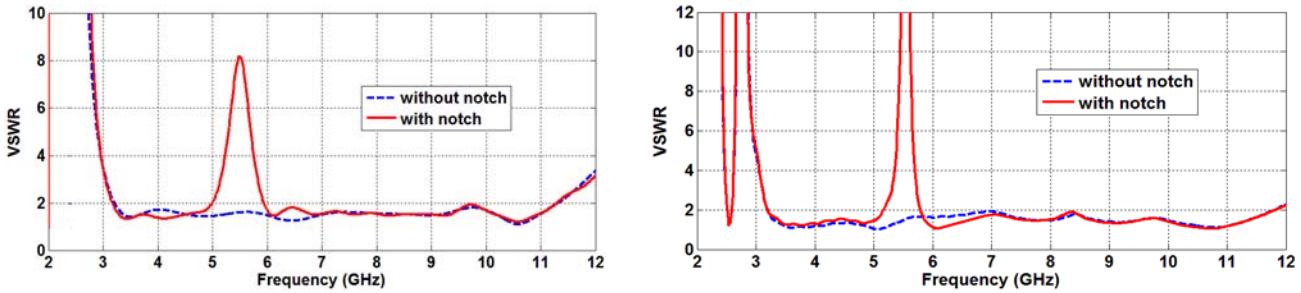

Figure 15. (a) Simulated VSWRs with and without band notch characteristics for (a) UWB design and (b) dual-band design.

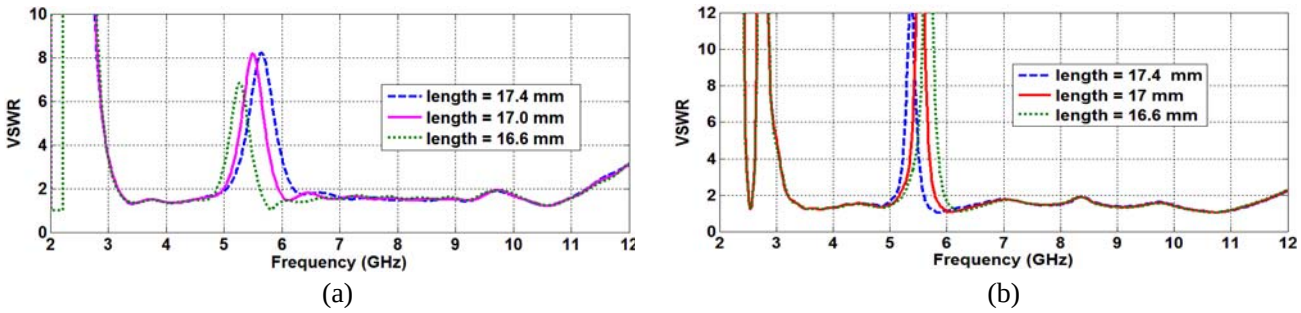

Figure 16. (a) Parametric variation of ring slot length and its effect on VSWR of the UWB design. (b) Parametric variation of ring slot length and its effect on VSWR of dual-band design.

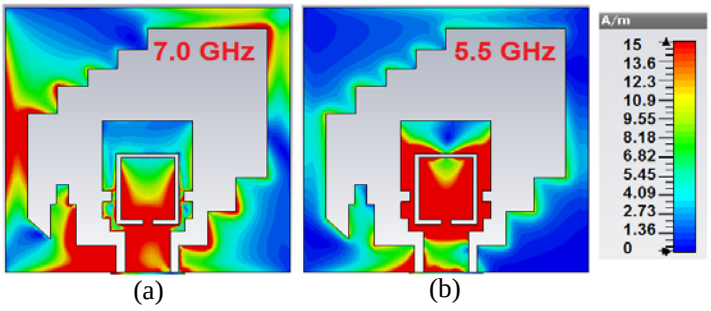

Figure 17. Current distribution for the UWB antenna at (a) outside the notch band frequency, 7.0 GHz and (b) within the notch band frequency, 5.5 GHz.

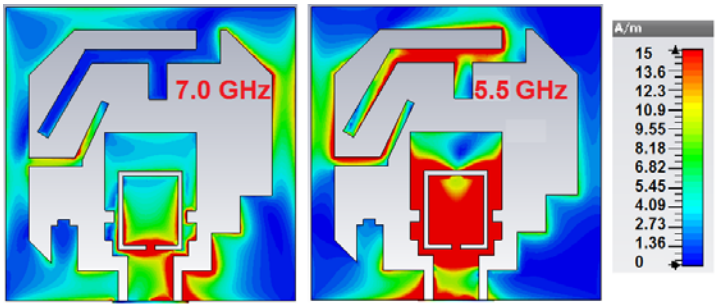

(a) (b)

Figure 18. Current distribution for the dual-band antenna at (a) outside the notch band frequency, 7.0 GHz and (b) within the notch band frequency, 5.5 GHz.

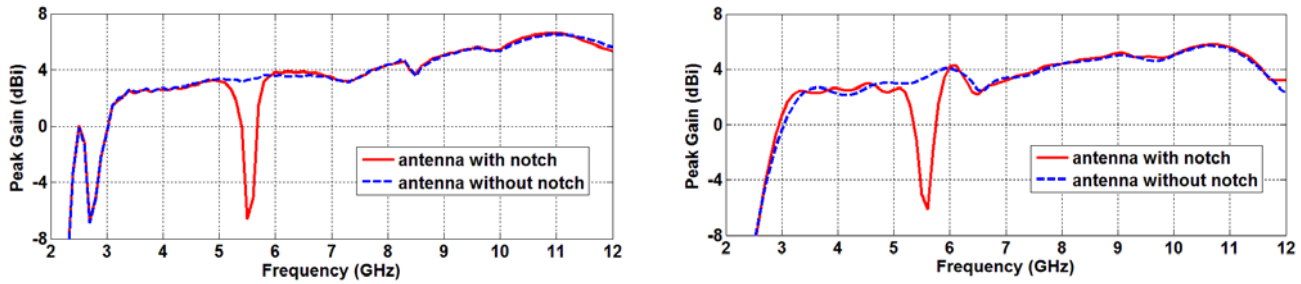

(a) (b)

Figure 19. (a) Peak gain of the proposed dual-band antenna with and without notch characteristics. (b) Peak gain of the proposed UWB antenna with and without notch characteristics.

and Figure 19(b) that the peak gains of the antenna with and without the notch characteristics are almost equal at all the frequencies except for the notch region. A sudden drop in the peak gain is observed at notched frequency due to non radiation of antenna at this band. The peak gain drops to as much as −4 dB indicating the capability of the antenna to suppress interference with the WLAN systems operating over this band.

8. CONCLUSIONS

Two compact CPW-fed antennas are proposed. One of the antennas is UWB (measured bandwidth being 3.4–11.2 GHz) while the other is dual band (measured bandwidth being 2.45–2.6 GHz and 3.2–11.6 GHz). The proposed antennas are fabricated on an FR-4 substrate and their performances measured. The measured results of the fabricated antennas show nearly omnidirectional radiation patterns over the entire operating band. The good impedance matching characteristics with measured gain acceptable for portable devices make these antennas a good candidate for LTE/WLAN/ WiMAX and UWB applications.

REFERENCES

1. FCC News, FCC 02-48, Feb. 14, 2002.
2. Lin, D.-B., I.-T. Tang, and M.-Y. Tsou, "A compact UWB antenna with CPW-fed," *Microwave and Optical Technology Letters*, Vol. 49, No. 3, 564–567, 2007.
3. Liu, W.-C. and W.-R. Chen, "CPW-fed compact meandered patch antenna for dual-band operation," *Electronics Letters*, Vol. 40, No. 18, 1094–1095, 2004.

4. Kim, T. H. and D. C. Park, "CPW-fed compact monopole antenna for dual-band WLAN applications," *Electronics Letters*, Vol. 41, No. 6, 291–293, 2005.
5. Lee, S. H., J. K. Park, and J. N. Lee, "A novel CPW-fed ultra-wideband antenna design," *Microwave and Optical Technology Letters*, Vol. 44, No. 5, 393–396, 2005.
6. Liu, W.-C., C.-M. Wu, and N.-C. Chu, "A compact CPW-fed slotted patch antenna for dual-band operation," *IEEE Antennas and Wireless Propagation Letters*, Vol. 9, 110–113, 2010.
7. De Cos, M. E., M. Mantash, A.-C. Tarot, and F. Las Heras, "Dual-band coplanar waveguide-fed smiling monopole antenna for WiFi and 4G long-term evolution applications," *IET Microwaves, Antennas & Propagation*, Vol. 7, No. 9, 777–782, 2013.
8. Thomas, K. G. and M. Sreenivasan, "Compact CPW-fed dual-band antenna," *Electronics Letters*, Vol. 46, No. 1, 13–14, 2010.
9. Li, Y. S., X. D. Yang, C. Y. Liu, and T. Jiang, "Compact CPW-fed ultra-wideband antenna with dual band-notched characteristics," *Electronics Letters*, Vol. 46, No. 14, 967–968, 2010.
10. Chu, Q.-X. and Y.-Y. Yang, "A compact ultrawideband antenna with 3.4/5.5 GHz dual band-notched characteristics," *IEEE Transactions on Antennas and Propagation*, Vol. 56, No. 12, 3637–3644, 2008.
11. Zehforoosh, Y. and T. Sedghi, "A CPW-fed printed antenna with band notched function using an M-shaped slot," *Microwave and Optical Technology Letters*, Vol. 56, No. 5, 1088–1092, 2014.
12. Zheng, Z.-A. and Q.-X. Chu, "Compact CPW-fed UWB antenna with dual band-notched characteristics," *Progress In Electromagnetics Research Letters*, Vol. 11, 83–91, 2009.
13. Krishna, D. D., M. Gopikrishna, C. K. Anandan, P. Mohanan, and K. Vasudevan, "CPW-fed Koch fractal slot antenna for WLAN/WiMAX applications," *IEEE Antennas and Wireless Propagation Letters*, Vol. 7, 389–392, 2008.
14. Zhao, G., F.-S. Zhang, Y. Song, Z.-B. Weng, and Y.-C. Jiao, "Compact ring monopole antenna with double meander lines for 2.4/5 GHz dual-band operation," *Progress In Electromagnetics Research*, Vol. 72, 187–194, 2007.
15. Kumar, R., P. V. Naidu, and V. Kamble, "Design of asymmetric slot antenna with meandered narrow rectangular slit for dual band applications," *Progress In Electromagnetics Research B*, Vol. 60, 111–123, 2014.
16. Kushwaha, N. and R. Kumar, "An UWB fractal antenna with defected ground structure and swastika shape electromagnetic band gap," *Progress In Electromagnetics Research B*, Vol. 52, 383–403, 2013.
17. Dawood, S. J., M. A. Salari, and O. H. Ghoochani, "Cross-slot antenna with U-shaped tuning stub for ultra-wideband applications," *International Journal of Antennas and Propagation*, Vol. 2008, Article ID 262981, 2008.
18. Sadat, S., M. Fardis, F. G. Geran, and G. R. Dadashzadeh, "A compact microstrip square-ring slot antenna for UWB applications," *Progress In Electromagnetics Research*, Vol. 67, 173–179, 2007.
19. Azenui, N. C. and H.-Y. D. Yang, "A printed crescent patch antenna for ultrawideband applications," *IEEE Antennas and Wireless Propagation Letters*, Vol. 6, 113–116, 2007.
20. Lee, J. N. and J. K. Park, "Compact UWB chip antenna design using the coupling concept," *Progress In Electromagnetics Research*, Vol. 90, 341–351, 2009.
21. Ma, T.-G. and C.-H. Tseng, "An ultrawideband coplanar waveguide-fed tapered ring slot antenna," *IEEE Transactions on Antennas and Propagation*, Vol. 54, No. 4, 1105–1110, 2006.
22. Dastranj, A. and M. Biguesh, "Broadband coplanar waveguide-fed wide-slot antenna," *Progress In Electromagnetics Research C*, Vol. 15, 89–101, 2010.
23. Mitra, D., D. Das, and S. R. Bhadra Chaudhuri, "Bandwidth enhancement of microstrip line and CPW-fed asymmetrical slot antennas," *Progress In Electromagnetics Research Letters*, Vol. 32, 69–79, 2012.
24. Dastranj, A. and H. Abiri, "Bandwidth enhancement of printed E-shaped slot antennas fed by CPW and microstrip line," *IEEE Transactions on Antennas and Propagation*, Vol. 58, No. 4, 1402–1407, 2010.

25. Chair, R., A. A. Kishk, and K.-F. Lee, "Ultrawide-band coplanar waveguide-fed rectangular slot antenna," *IEEE Antennas and Wireless Propagation Letters*, Vol. 3, No. 1, 227–229, 2004.
26. Liang, J., C. C. Chiau, X. Chen, and C. G. Parini, "Study of a printed circular disc monopole antenna for UWB systems," *IEEE Transactions on Antennas and Propagation*, Vol. 53, No. 11, 3500–3504, 2005.
27. Zhan, K., Q. Guo, and K. Huang, "A miniature planar antenna for Bluetooth and UWB applications," *Journal of Electromagnetic Waves and Applications*, Vol. 24, No. 16, 2299–2308, 2010.
28. Yildirim, B. S., B. A. Cetiner, G. Roquetra, and L. Jofre, "Integrated Bluetooth and UWB antenna," *IEEE Antennas and Wireless Propagation Letters*, Vol. 8, 149–152, 2009.
29. Tao, J., C. H. Cheng, and H. B. Zhu, "Compact dual-band slot-antenna for WLAN applications," *Microwave and Optical Technology Letters*, Vol. 49, No. 5, 1203–1204, 2007.
30. Wu, J.-W., H.-M. Hsiao, J.-H. Lu, and S.-H. Chang, "Dual broad-band design of rectangular slot antenna for 2.4 and 5 GHz wireless communication," *Electronics Letters*, Vol. 40, No. 23, 1461–1463, 2004.
31. Mishra, S. K., R. Gupta, A. Vaidya, and J. Mukherjee, "Printed fork shaped dual band monopole antenna for Bluetooth and UWB applications with 5.5 GHz WLAN band notched characteristics," *Progress In Electromagnetics Research C*, Vol. 22, 195–210, 2011.
32. Tsai, L.-C., "A triple-band bow-tie-shaped CPW-fed slot antenna for WLAN applications," *Progress In Electromagnetics Research C*, Vol. 47, 167–171, 2014.